Signal, Image and Video Processing
https://doi.org/10.1007/s11760-024-03450-4

ORIGINAL PAPER

Cost effective detection of uneven mounting fault in rotary wing drone motors with a CNN based method

Nurdoğan Ceylan[1] · Eyup Sönmez[2] · Sezgin Kaçar[3]

Received: 24 April 2024 / Revised: 11 June 2024 / Accepted: 18 July 2024

Abstract
Rotary wing drones stand out among Unmanned Aerial Vehicles with their vertical landing and take-off feature and are used in many industrial applications and different sectors. Ensuring the stability of motion in these vehicles is crucial. Errors in the motor assembly can disrupt the stability of the motion in rotary wing drones. Therefore, it is essential to detect these errors during the assembly phase. In this study, we propose a cost-effective method based on deep learning to detect assembly failure of brushless direct current motors, which are widely used in rotary wing drones. A test setup representing the motor assembly defects is created and vibration data for three different speeds of the motor are obtained through a low-cost vibration sensor. The combined one- and two-dimensional deep convolutional neural network (WDD-CNN), used to classify these data was trained with the Case Western Reserve University (CWRU) dataset and the data collected in this study. The hyper-parameter settings of the network were determined using the CWRU data set and the data obtained from the experimental setup described in the paper. The network parameters of the WDD-CNN network were transferred to the Raspberry Pi micro-controller with specialized software, and the classification process was performed there. The fact that the proposed method runs on a micro-controller reduces its cost. Because there is already a micro-controller card in drones. In addition, the selected sensor is cost-effective. Thanks to these features, the proposed method is cost effective. In this classification process performed on Raspberry Pi 5, assembly errors were detected with 97–100% accuracy.

Keywords Rotary wing drone · BLDC Motor · CNN · MEMS sensor · Deep learning

1 Introduction

The use of unmanned aerial vehicles (UAVs) has become increasingly prevalent in recent years [1]. It significantly reduces the time required for business processes in numerous sectors, resulting in notable benefits [2]. UAVs are categorised according to their wing structure: fixed wing and rotary wing. Rotary-wing UAVs eliminate the need for long runways with their vertical landing-take-off feature. In this way, they can be used more easily in residential areas with long runway restrictions, such as city centers. Brushless DC motors are preferred in these drones due to their advantages, including quiet operation, longevity, and ease of maintenance [3, 4]. These motors are mounted on the wings of drones, and the movement of these motors enables flight [5]. The accurate mounting of the motors is the primary factor influencing the stability of the drone's motion [6]. An incorrectly mounted motor will result in unusual vibrations, which can cause bearing failures, shaft fractures, rotor failures, and broken motor mounting feet. Most UAV malfunctions and accidents are caused by motor failures [7]. Such failures have the potential to disrupt the stability of the drone's motion, leading to accidents and resulting in significant losses of both work and equipment. To avoid this situation, it is of great importance to apply effective methods for detecting uneven mounting faults.

Eyup Sönmez and Sezgin Kaçar have contributed equally to this work

✉ Eyup Sönmez
d175045051@subu.edu.tr

Nurdoğan Ceylan
nceylan@adiyaman.edu.tr

Sezgin Kaçar
skacar@subu.edu.tr

[1] Mechanical Engineering, Adıyaman University, 02040 Adıyaman, Turkey

[2] Mechatronics Engineering, Sakarya University of Applied Sciences, 54100 Sakarya, Turkey

[3] Electrical and Electronics Engineering, Sakarya University of Applied Sciences, 54100 Sakarya, Turkey

Published online: 12 August 2024

1.1 Related works and research gap

There are many deep learning and machine learning-based methods for fault detection in the literature. Kilic and Unal [8, 9] detected malfunctions in the angle of attack sensor and pitot probes and static ports, which are components of commercial aircraft, using machine learning methods. In addition, Kaya et al. [10], Akcan et al. [11] proposed machine learning and deep learning methods for fault detection in bearings.

Glowacs [12] has performed fault detection using audio signals in an induction motor. Three different faults and normal condition of an induction motor are classified. Data was preprocessed with two different feature extraction methods and classified with three different Machine Learning (ML) methods. Glowacz et al. in this work, [13] detected fault in single-phase induction motors using sound signals. Normal condition and three different faults are classified with three ML based classifiers. Ameid et al. [14] have detected different faults of induction motors by analyzing FFT technique. Different mechanical and electrical quantities (rotor speed, quadratic current components, and stator phase current) were used in the analysis. Hosseini et al. [15] have detected, stator inter-turn fault in brushless direct current (BLDC) motors. For this purpose, stator current data was obtained simulatively. These data were analyzed with the discrete wavelet transform method and the fault was detected. Tian et al. [16] evaluated fault detection studies with artificial intelligence and signal processing methods in asynchronous motors. They stated that acoustic, vibration, current and voltage data are generally used in these studies. Hernandez et al. [17] proposed a method based on quaternion signal analysis for asynchronous motor fault detection. They used accelerometer data in their study. They used tree classification method as the classification method. Ali et al. [18] detected different mechanical and electrical faults of asynchronous motors using machine learning methods. They used stator currents and vibration data as data. Signal processing methods were used for feature extraction and machine learning methods were used for classification. The study of Al Shorman et al. [19] provides a review of studies to detect and monitor bearing, rotor and stator failures (and their combinations) in asynchronous motors based on sound and acoustic emission data. Lee et al. [20] conducted an experimental study on the detection of asynchronous motor errors. They classified the vibration data they collected using CNN. Chang et al. [21] detected asynchronous motor malfunctions by examining the vibration and electrical data they collected with data analysis methods. Abed et al. [22], classified four bearing states in a BLDC motor after feature extraction by various methods using a recurrent neural network (RNN). Shifat et al. [23], extracted various features in time and frequency domains from sensor signals. And used an artificial neural network (ANN) to classify three health states of the motor.

In addition to these studies, some deep learning and machine learning-based methods have been proposed in the literature to detect BLDC motor faults directly used in UAVs. Lee et al. [24], proposed a mathematical model to detect BLDC motor faults used in UAVs. They used electrical data to detect faults. Bondyra et al. [25], presented a method for detecting physical defects of UAV rotor blades. The data used is based on acceleration measurements from the IMU (Inertial Measurement Unit) sensor. SVM was used as a classifier. Pourpanah et al. [26], developed a monitoring system that can detect possible malfunctions in UAV engines and propellers early. Faults were classified using machine learning methods using vibration and current data. V. Medeiros et al. [27], described a chaos-based signal processing method to analyze BLDC motor behavior used in drones. Current was used as data. Iannace et al. [28], used NN to detect stability faults in BLDC motors used in UAVs with 97–98% accuracy. Magdaleno et al. [29], analyzed audio signals with DWT and Fourier Transform methods. Thus, propeller failures in BLDC motors were detected. Veras et al. [30], detected eccentricity fault in BLDC motors by decomposing the obtained sounds signals with wavelet multiresolution analysis and a chaos-based method. Liu et al. [31], converted sound signals into images with time–frequency analysis methods to detect propeller faults in BLDC motors and classified these spectrogram images with CNN. Altinors et al. [32] extracted statistical features of the signals obtained from propeller, eccentric and bearing faulty motors and classified them using DT, SVM and KNN machine learning algorithms. Yaman et al. [33], classified different faults of BLDC motors (balance fault, magnet fault, bearing fault and propeller fault) with SVM using audio signals.

The aim of this study is to develop a deep learning-based cost-effective method that can work in real-time to detect uneven mounting defects in BLDC motors, which are widely used in rotary wing UAVs. According to the literature review, no study is found for the detection of uneven mounting defects in BLDC motors used in drones. This represents a significant research gap, as the reliable and efficient detection of such defects is crucial for the performance and safety of UAVs.

In the literature, there are machine learning and deep learning based methods for fault detection in BLDC motors used in drones [28, 31]. However, many of these machine learning methods require specialized feature extraction processes, which can be complex and time-consuming. The proposed WDD-CNN network performs high accuracy fault detection by processing raw data, eliminating the need for complex feature extraction [34]. In addition, both the low cost of the sensor used and the use of micro-controllers for classification processes significantly reduce the cost of fault detection.

Micro-controllers, being compact and efficient, offer a practical solution for real-time classification, making the system both cost-effective and suitable for real-world applications. The performance of the proposed system is measured in a test setup where an uneven mounting defect is modeled. Accordingly, the proposed system detects uneven mounting defects with accuracies ranging from 97–100%.

2 Methods and materials

2.1 Methods

In this study, a test setup has been created to detect uneven mounting defects of BLDC motors used in drones. In this test setup, the vibrations generated by the motor are picked up by a vibration sensor and transferred to the Raspberry Pi 5 microcontroller. A deep learning network, which was previously created on the Raspberry to detect motor faults, determines whether the mounting of the motor is faulty from this data. These process steps are shown in Fig. 1.

As a first step, 2000, 4000 and 6000 rpm vibration signals were collected from the relevant test setup, respectively, using the Micro Electro Mechanical System (MEMS), a cost-effective vibration sensor. A new data set was created by combining the collected signals separately and respectively with the 1 hp, 2 hp and 3 hp vibration signals of the 0.007 inch CWRU data set. In the next step, the first group of vibration data is reserved for training, and the second and third group of vibration data are reserved for testing. The raw vibration data allocated for training was reproduced by applying the sliding window method. The test data is left in its original form. In the next stage, both training and test data were subjected to normalization. After the normalization process, the sensor data allocated for training and testing were converted into one-dimensional and two-dimensional training and test samples, each consisting of 3600 dijital signals. Model training was carried out using the WDD-CNN model with training samples and model weights were obtained. The trained model was transferred to the embedded system, the model was tested with test samples, and the results were taken as a confusion matrix.

2.1.1 Convolutional neural networks-CNNs

Convolutional neural networks (CNN) are simple neural networks that use convolution in at least one of their layers [35]. Convolution is a kind of linear operation and is defined mathematically in Eqs. (1) and (2). A CNN network structure basically consists of convolution layer, pooling layer and fully connected layer components. The general layer structure of CNN networks is shown in Fig. 2. It shows the typical structure of a CNN with several basic layers. The input layer is the first layer where data is fed into the network. Then comes the convolution layer. In this layer, a special mathematical operation called convolution is performed by shifting a filter matrix over the input data in certain steps. The result is a smaller output matrix called a feature map. This output matrix is fed into a ReLu activation function and transferred to the accumulation layer. Here again, a selected smaller kernel is shifted over the output matrix of the convolution layer and the operations required by the selected pooling function (max. pooling, average pooling, etc.) are performed. The figure shows the max pooling operation of a 2x2 kernel. The output of the pooling layer is then usually fully connected layers. These layers are usually followed by a softmax activation function. This function returns the probability values for the classes in a classification problem. All these processes are shown schematically in Fig. 2.

The fully connected layer is structured in the same way as the FCL in a standard feedforward neural network and has a similar function. The advantages of CNN stem from the structural and functional distinctions between Convolutional Layers (CLs) and Pooling Layers (PLs) [36]. The main difference of CLs from connected layers is that densely connected layers learn general properties, whereas convolutional layers learn local properties [35].

A CL consists of a number of structures defined as learning cores. Each core has a trainable weight and a bias. The input data is convolutionalized in the CL layer and the result of the convolutional operation is fed to an activation function. The output of this activation function is the final output of CL [37]. Equation (1) mathematically describes the function of the convolution layer (1-D). Equation (2) describes the function of the convolution layer (2-D).

$$X_l^n = \sum_{c=1}^{C} \left(X_{l-1}^c * W_l^{(c,n)} \right) + B_l^n \tag{1}$$

$$X_l^n(i,j) = \sum_{c=1}^{C} \left(\sum_{m=0}^{M-1} \sum_{n=0}^{N-1} X_{l-1}^c(i+m, j+n) \cdot W_l^{(c,n)}(m,n) \right) + B_l^n \tag{2}$$

In Eq. (1), * denotes the convolution process. X_l^n represents the nth feature map at the l-th layer. X_{l-1}^c corresponds to the c-th channel in the input filter dimensions in the (l-1)-th layer. $W_l^{c,n}$ is the nth weight matrix of channel c in layer l. B_l^n is the nth bias matrix at layer l. The most frequently used activation function in CNNs is ReLU (Rectified Linear Unit). Returns the same value when the function is given a positive input value, and zero when given a negative input value. Compared with ReLU, sigmoid or similar functions, it speeds up the CNN training process and eliminates the vanishing gradient problem [38]. Equations (3) and (4) define

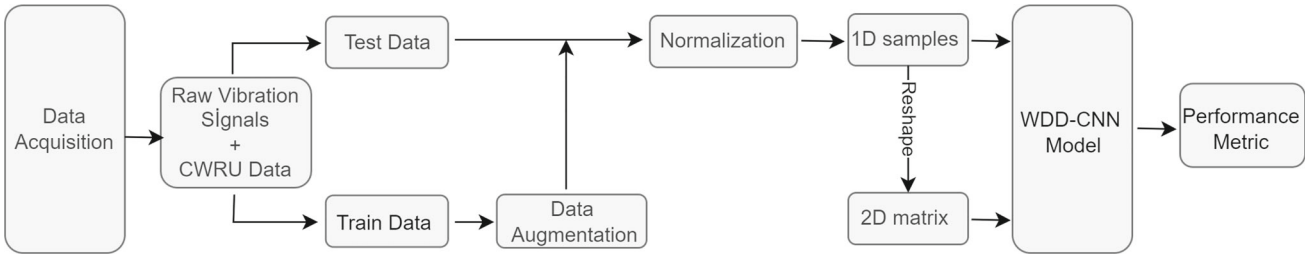

Fig. 1 Process steps of WDD-CNN network

the 1-D and 2-D ReLU function.

$$X_l^n(i) = \max\left(0, X_{l-1}^n(i)\right) \tag{3}$$

$$X_l^n(i,j) = \max\left(0, X_{l-1}^n(i,j)\right) \tag{4}$$

CNNs usually have a PL after the CL. The purpose of PL is to reduce the size of the feature maps created by the previous layer. Following the convolutional layer, the pooling layers perform a down sampling procedure to remove redundant information. It also reduces computational cost as the input size is reduced. Equations (5) and (6) are the mathematical functions of 1-D and 2-D pooling layer.

$$X_l^n(i) = \underset{r=i}{i+R-1}\left(X_{l-1}^n(r)\right) \tag{5}$$

$$X_l^n(i,j) = \underset{r=i}{\overset{i+R}{\max}}\left(\underset{s=j}{\overset{s+J}{\max}}\left(X_{l-1}^n(r,s)\right)\right) \tag{6}$$

The mentioned layers are combined in various ways to create many different deep learning methods.

2.1.2 Transfer learning and WDD-CNN network used

Transfer learning is the approach of using pre-trained deep learning networks with large datasets to solve a new problem. Using a pre-trained network is a common method when there is not enough data to train the network. This eliminates the need for a large data set to train the network and reduces processing costs. The size and variety of the data set used to train these networks allows them to adapt easily to new problems.

Deep learning and transfer learning methods remain popular for fault detection of electric motors. These methods can work with different types of data such as vibration, current, voltage and sound data. In this study, vibration signals collected from BLDC motor and CWRU dataset are used together for fault detection. Vibration signals are commonly used time series data for intelligent fault detection. These data provide valuable information about the operating state of motors, enabling the detection of various types of faults [39, 40].

Methods based on deep learning are generally categorized into two aspects: methods that work on one-dimensional signals such as time series data and those that reshape one-dimensional input signals into two dimensions [41]. The 2D-CNN architecture, which works on two-dimensional data, is capable of capturing both spatial and temporal relationships in the data, while the 1D-CNN architecture, which works on one-dimensional data, has advantages such as overfitting and scaling invariance. In this study, we integrate the advantages of 1D-CNN and 2D-CNN methods for BLDC motor fault detection. A WDD-CNN model is used in [34] for real-time condition monitoring and early fault detection of electric motors under noisy and changing operating conditions. The hyper-parameter settings of this network are reconfigured to categorize a 2-class data set. Thus, the data obtained from the BLDC motor in the experimental set were categorized as faulty and normal. Figure 3 represents the architecture of this network.

2.2 Materials

The test setup used in this study (see Fig. 4) consists of a sample drone motor (A2212/10T 1400 KV)(Image 1 in Fig. 4b), ADXL-345 Micro Electromechanical System (MEMS) sensor (accelerometer)(Image 3 in Fig. 4b), motor driver (Image 2 in Fig. 4b), Raspberry Pi 5 micro-controller (Image 4 in Fig. 4b)and 0–30 V DC power supply (Image 6 in Fig. 4b). In addition, the hyper-parameter settings of the deep learning network used in classication are made on MSI Bravo 15C7V PC with AMD Ryzen 5 7535HS with Radeon Graphics 3.30 GHz processor (Image 7 in Fig. 4b). Image 5 in Fig. 4b represents the tachometer used to measure BLDC motor speed.

2.2.1 BLDC motor and driver

Brushless Direct Current (BLDC) motors have become rapidly popular in recent years. BLDC motors are used in sectors such as aerospace, medical, industrial automation equipment, especially in white goods and automotive [42]. And it is thought to replace brushed DC motors in the near future. Especially the widespread use of electric cars

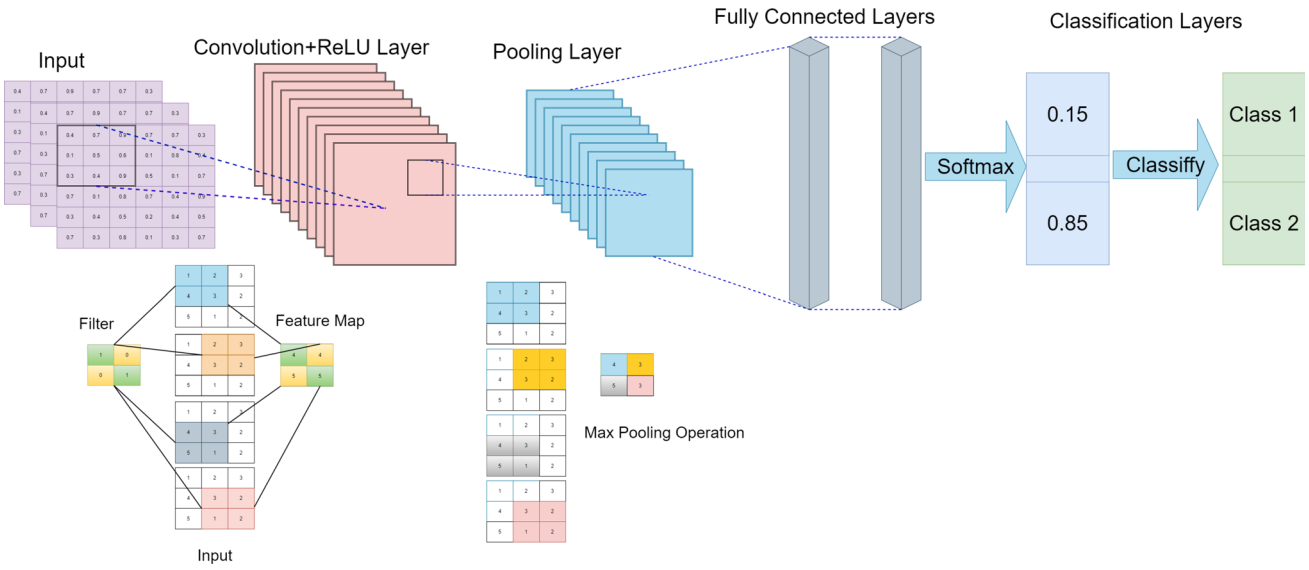

Fig. 2 CNNs layer structure

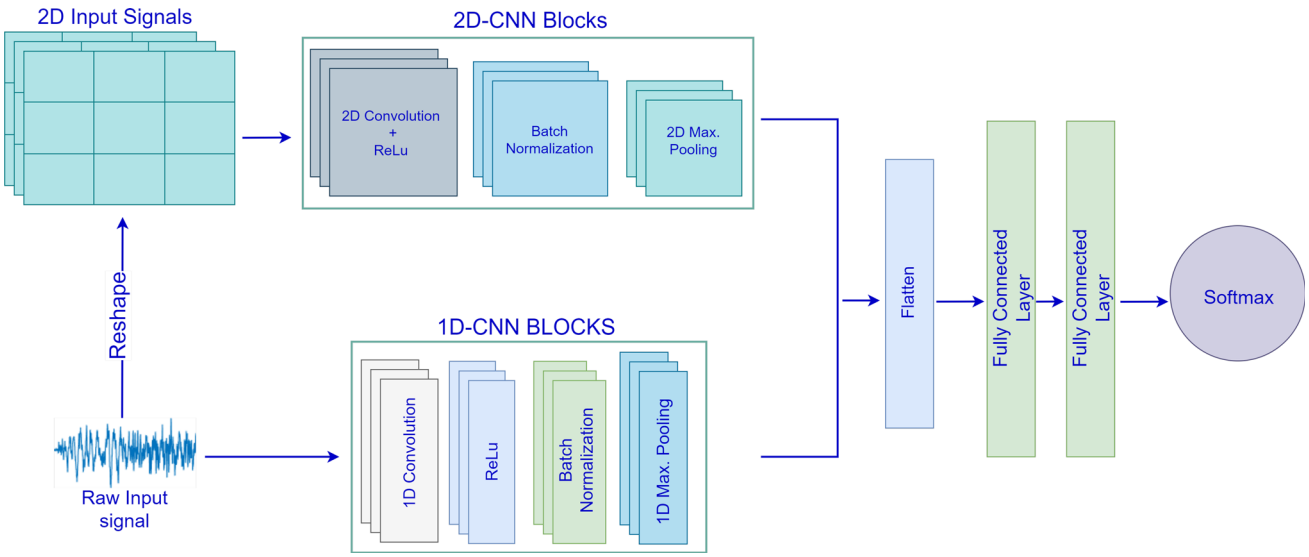

Fig. 3 The architecture of WDD-CNN network

is expected to significantly increase the demand for BLDC motors. In 2025, the economy generated by BLDC motors is estimated to be 15.2 billion dollars [43].

BLDC motors are electronically commutated instead of brushes. BLDC motors have many advantages over brushed DC motors and induction motors. A few of these are: High efficiency, better torque characteristics, more dynamic response, longer operating life, quiet operation, wider speed ranges. In addition, these motors provide higher torques compared to the size of the motor. This makes them useful in applications where space and weight are critical factors [42]. The A2212/10T 1400KV BLDC motor shown in Fig. 4a is used in this study. Figure 4b shows a schematic representation of this motor and the experimental set. This motor weighs approximately 50 g and measures 27.5 × 30 mm. It rotates its shaft 1400 revolutions per minute per volt without propeller. Its maximum efficiency is 80% and the current it draws at maximum efficiency is 4–10 A. The operating voltage is 11.1 V. "Cyclic Collective Pitch Mixing (CCPM) servo consistency master" driver is used to run this motor at varying speeds. The CCPM servo system is developed to enable three servo motors to react simultaneously and at the same speed. However, in the experimental set, only one of these three outputs is used to drive the BLDC motor in the set. Figure 4a shows the CCPM servo consistency master drive and Fig. 4b shows a schematic representation of the driver.

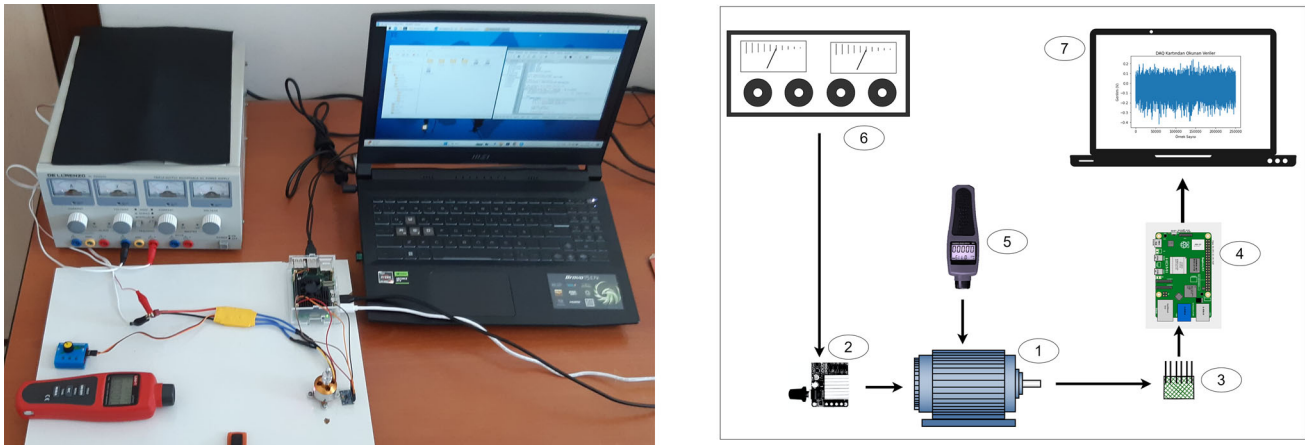

(a) The Test Setup

(b) Schematic Representation of Test Setup

Fig. 4 The test setup and schematic representation of the test setup

2.2.2 ADXL345 accelerometer

Adafruit's ADXL-345 Micro Electro Mechanical System (MEMS) accelerometer was used in this study. The sensor is a triaxial accelerometer measuring $3 \times 5 \times 1$ mm and is shown in Fig. 4a shows the accelerometer and Fig. 4b number 3 shows a schematic representation of the ADXL345 accelerometer. In the ADXL-345, acceleration data can be accessed via I2C and SPI protocols. This data passes through a 13-bit Analog Digital Converter (ADC) before being transmitted. Furthermore, the measurement range ranges from ± 2, ± 4, ± 8 and ± 16 g and is user selectable. The sampling frequency of the sensor ranges from 0.1 Hz to 3.2 kHz [44].

The frequency response (in Hz) of the ADXL345 accelerometer is defined by the bandwidth of the accelerometer, which in turn is determined by the output data rate (ODR). The maximum available bandwidth of ADXL345 is 1600 Hz [45, 46]. This means that the accelerometer can accurately measure vibrations and movements up to this frequency. When the technical specifications of the ADXL345 accelerometer are examined, it is seen that it has an A/D digital converter and digital filter. Therefore the ADXL345 accelerometer is ready to be used to detect vibration in electric motors [47]. The A2212/10T 1400 KV motor, which is widely used in drones and other RC applications, has 14 poles. These motors reach frequencies of approximately 235, 465 and 600 Hz at 2000, 4000 and 6000 rpm, respectively. Soft foot (Looseness-Uneven mounting) errors typically occur at speeds of $1\times$ the motor's operating speed (base frequency) [48]. However, higher harmonics may also occur due to the nature of the fault. Therefore, the ADXL345 vibration sensor is capable of capturing the harmonics of the relevant BLDC motor.

2.2.3 Raspberry Pi 5

Raspberry Pi is a low-cost, compact and portable microcontroller. It can be connected to devices such as a computer screen, television, keyboard, mouse and external memory units. The Raspberry Pi can be programmed in Scratch or Python. It comes with a Linux-based operating system called Raspberry OS installed [49].

A powerful feature of the Raspberry Pi is a 40-pin GPIO (general purpose input/output) pinout that runs along the top edge of the board. The Raspberry Pi 5 is up to three times faster than its predecessor, making it useful for powerful applications. Raspberry Pi 5 was used for the developed system. This model comes with 8 GB of RAM, 2.4 GHz quad-core 64-bit Arm Cortex-A76 CPU, VideoCore VII GPU supporting OpenGL ES 3.1, Vulkan 1.2 and other functions. It has built-in Wi-Fi and Bluetooth capabilities. It also allows SPI and I2C serial communication. The Raspberry Pi 5 and connections used in the test setup are given in Fig. 4a. Figure 4b number 4 shows a schematic representation of the micro-controller.

3 Experimental results

3.1 Data set

The data set used in training the WDD-CNN network used in this study was obtained by combining the Case Western Reserve University (CWRU) data set with the data set obtained from the test setup shown in Fig. 4. CWRU data set is a reference data set in motor fault detection studies and bearing fault detection studies [50].

Data was collected from two different ends of the test motor (fan-end, drive-end), at 12 kHz and 48 kHz frequencies, by first installing normal bearings and then by installing bearings with defects of different sizes (0.007, 0.014, 0.021, and 0.028 inches). In addition, these data were collected again for different load cases (1hp, 2hp and 3hp). In this study, data collected from normal bearings under 1hp, 2hp, 3hp loads at 48 kHz frequency were used.

The data shown in Fig. 4 was collected with the ADXL-345 MEMS accelerometer mounted right next to an uneven mounted BLDC motor and transferred to Raspberry Pi 5. The data was recorded for 500 s. There are approximately 250,000 numerical values in each recorded piece of data. Data were collected under motor speeds of 2000 rpm, 4000 rpm and 6000 rpm.

MEMS sensors are cost-effective vibration sensors that can collect digital data from three axes, X, Y and Z axes. However, removing axis data that do not contribute to model training positively affects model performance. Data that carry less information and therefore do not contribute to model training can be identified by analyzing the mean, standard deviation and amplitude values [51–53]. In our study, the mean, standard deviation and amplitude values of the collected three-axis digital vibration data were analyzed. As a result of the analysis, it was observed that the Z-axis data had less variance. For this reason, X and Y axis data were used for model training in our study.

Figure 5a shows the normal data (from CWRU), (b) shows X-axis signals of the accelerometer data recorded while the motor was rotating at 6000 rpm.

3.1.1 Training data set

The content of the data used in training the WDD-CNN network is given in Table 1. Accordingly, normal data were taken from the data of the CWRU data set collected under 1 hp load at 48 kHz sampling frequency. Uneven mounting data was obtained from the no propeller rotation of the motor at 2000 rpm in the BLDC test set created within the scope of this study.

These data are increased by data augmentation. Data augmentation is the process of artificially increasing the amount of data using different methods. Deep learning models require large amounts of data during the training process. However, this is often costly and difficult. Therefore, increasing training data, data augmentation is often done in deep learning studies. In this study, the sliding window method, which is an effective and easy method for time series, is used.

The sliding window technique enables data augmentation by moving a fixed-size window across the data, creating multiple overlapping samples. Given a 1D input sequence and a window size, the sliding window operation generates multiple segments of the sequence. 1D Sliding Window Mathematical Representation is explained below:

1D input sequence:

$$x = [x_1, x_2, x_3, \ldots, x_n] \tag{7}$$

The augmentation process:

$$y_i = [x_{(i-1)s+1}, x_{(i-1)s+2}, \ldots, x_{(i-1)s+w}] \tag{8}$$

where

- y_i is the i-th augmented segment.
- w is the window size.
- s is the step size.
- The index i ranges from 1 to $\left\lfloor \frac{N-w}{s} \right\rfloor + 1$, ensuring each window fits within the bounds of the input sequence x.

According to this method, the window length was selected as 3600 and this window is shifted in steps of 128, creating a total of 3900 data of 3600*1 size, 1950 of which were faulty and 1950 are normal. In this way, the training data is increased approximately 30 times (see Table 2).

3.1.2 Test data set

The main purpose of this study is to detect the uneven mounting fault of an uneven mounted BLDC motor. For this purpose, a test setup representing an uneven mounting fault is created and data is collected for different speeds of the motor. The network proposed in [34] has been proven to be successful in detecting faults from raw data. For this reason, the test data created in this study is created by recording the data collected while the BLDC motor was rotating at different speeds without processing it. Accordingly, raw data with dimensions of 250,000*1 are recorded for 500 s while the engine is rotating at 4000 rpm and 6000 rpm. These data are divided into 3600 equal parts and 69 4000 rpm and 69 6000 rpm data are created. The normal data of the test data set is taken from CWRU's data under 48 kHz sampling frequency, 2 hp and 3 hp load. Faulty data collected at 4000 rpm and normal data collected under 2 hp load were classified in the experiment 1. The test data set is stated in Table 3. The faulty data are collected at 6000 rpm and the normal data are collected under 3 hp load are classified in the experiment 2. The test data set used in the experiment 1 is named Dataset A, and the test data set used in the experiment 2 is named Data Set B.

3.2 Experiments

In Experiment 1, Dataset A is classified. Accordingly, the normal data of the CWRU data set (48 kHz, 2 hp) and the

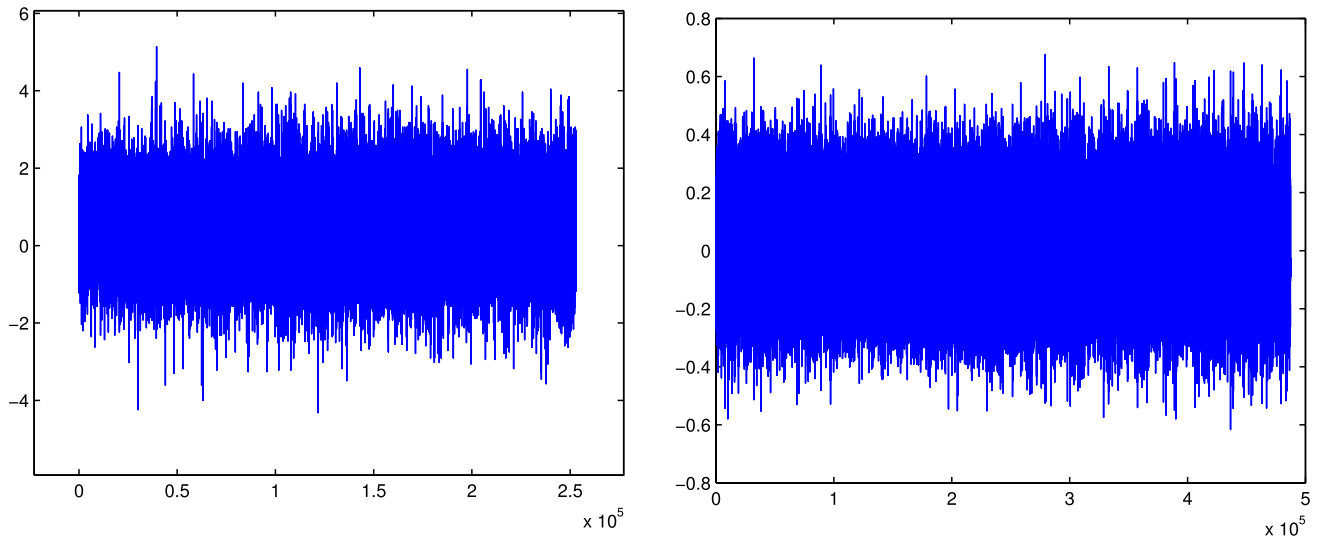

(a) An example signal from the setup data set

(b) An example signal from the CWRU data set

Fig. 5 The test setup and schematic representation of the test setup

Table 1 Content of training data

	Normal	Uneven mounting
Data parts	CWRU data set	The BLDC test set
Features	Sampling frequency, 48 kHz	BLDC motor speed, 2000 rpm
	Load 1 hp	No propeller

Table 2 Training data set

	Normal data (from CWRU)	Uneven mounting data (from setup)	Training data set
Number	1950	1950	3900
Dimensions	3600*1	3600*1	3600*1

vibration data obtained from the incorrectly mounted BLDC motor in the setup created within the scope of the study while rotating at 4000 rpm are classified. Accuracy, recall, precision and F score metrics are chosen to measure classification performance. The equations for these metrics are given in Eqs. 9, 10, 11, 12.

$$\text{Accuracy} = \frac{\text{TP} + \text{TN}}{\text{TP} + \text{FN} + \text{FP} + \text{TN}} \tag{9}$$

$$\text{Precision} = \frac{\text{TP}}{\text{TP} + \text{FP}} \tag{10}$$

$$\text{Recall} = \frac{\text{TP}}{\text{TP} + \text{FN}} \tag{11}$$

$$F1 - \text{score} = 2 \times \frac{\text{Precision} \times \text{Recall}}{\text{Precision} + \text{Recall}} \tag{12}$$

Here TP: True Positive, TN: True Negative, FP: False positive and FN: False Negative. Accuracy: It refers to the ratio

Table 3 Test data set

		Features	Number	Dimensions	Total
Dataset A	Normal data 1 (from CWRU)	48 kHz, 2 hp	69	3600*1	138 Test data samples
	Uneven mounting data 1 (from setup)	4000 rpm	69	3600*1	
Dataset B	Normal data 2 (from CWRU)	48 kHz, 3 hp	69	3600*1	138 Test data samples
	Uneven mounting data 2 (from setup)	6000 rpm	69	3600*1	

Table 4 Experiments's results

Experiments	Accuracy (%)	Recall	Precision	F1 Score
Experiment 1	100	1	1	1
Experiment 2	100	1	1	1

of correct predictions to all predictions. Precision is the ratio of correctly predicted positive cases to all positive predictions. Recall shows the ratio of correctly predicted positive cases to all predictions belonging to a class. F1 score is the weighted average of precision and recall. The results of these metrics are shown in Table 4. The results of these metrics are shown in Table 4.

In Experiment 2, Dataset B was classified. Accordingly, the normal data of the CWRU data set (48 kHz, 3 hp) and the vibration data obtained from the uneven mounted BLDC motor in the setup created within the scope of the study while rotating at 6000 rpm are classified. Figure 6 shows the confusion matrices of Experiment 1 and Experiment 2.

The confusion matrices of Experiment 1 and Experiment 2 have to be explained in detail. Response: According to the confusion matrix given in Fig. 6, 138 samples were tested. Of these, 69 samples represent the positive class and 69 the negative class. In both experiment 1 and experiment 2, all samples were correctly predicted. In this case, the number of correctly predicted positive examples will be 69 and the number of correctly predicted negative examples will be 69 (TP = 69, TN = 69). Therefore, the accuracy metric will be 100% and the other metrics will be 1 (Table 4).

4 Discussions

According to our research, there has been no previous study trying to detect uneven mounting defects in drone motors with a deep learning-based method. Yaman et al. at their work [33], a machine learning-based method proposed for bearing fault, propeller fault, unbalance situation and magnet failure. The method proposed here differs from this study both in terms of the faults examined and the method used. However, it can be compared to this study under the common title of detecting BLDC motor faults used in drones with an artificial intelligence based method. They used computers to train machine learning methods and detect the faults. In the method proposed within the scope of this study, the computer was used only in training the network proposed with new data, and the classification was performed on the microcontroller. In this way, the proposed method can be easily adapted to faulty situations that may arise during the flight of UAVs. The method proposed in this study can be used both in flight and in ground tests. Computer-controlled methods are more suitable for ground tests. Additionally, using a micro-controller for classification is less costly. Because UAVs already have a micro-controller used to control all electronic systems of the vehicle. This micro-controller can also be used for fault detection, so it does not require an additional micro-controller cost. It is a fact that the proposed method has aspects that are better than other studies, but also aspects that need improvement. The proposed model addresses the uneven mounting fault by completely separating it from other faults that may have vibration defects. For example, some vibrations may occur during flight due to weather conditions. Motor defects such as bearing defects and unbalance situations that may accompany mounting faults also create vibrations, and these vibrations are also worth examining. It is thought that the proposed method will also detect these vibration defects as faults. In future studies, these different fault sources will be combined and examined. In the literature, since bearing defect and unbalance fault in BLDC motors can be detected with effective methods, [5, 22], have primar-

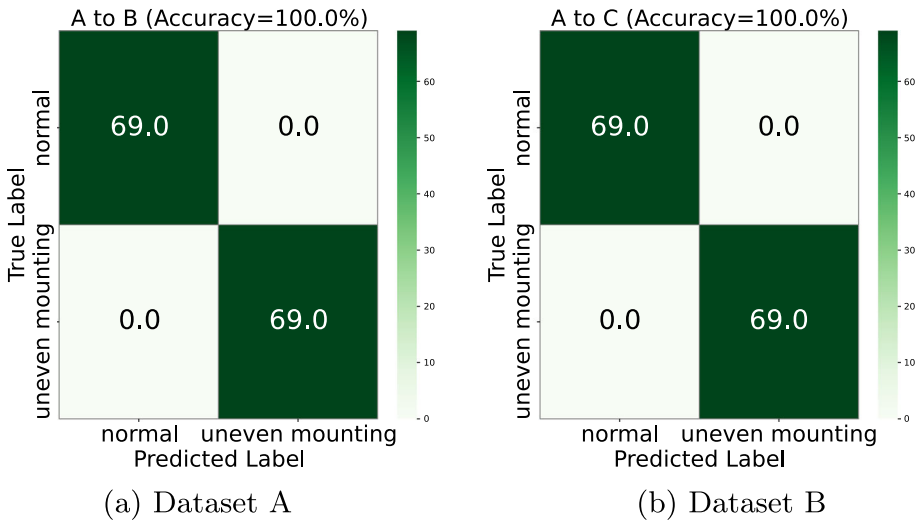

(a) Dataset A (b) Dataset B

Fig. 6 Confusion matrixes of dataset A and dataset B

ily focused on uneven mounting fault. Another area open to development is the use of data augmentation method in training data. Although data augmentation is widely used in deep learning studies, these synthetic signals created through data augmentation may cause some limitations in reflecting real conditions. No processing is applied to the data in the test data set. However, data augmentation is performed in the training data set.

5 Conclusions

In this study, a deep learning-based model is proposed to detect uneven mounting defects of BLDC motors used in UAVs. It is known that the proposed network detects faults in electric motors with high accuracy. This network was also used in the test setup created within the scope of this study, where the uneven mounting fault of BLDC motors is tested, and the results are examined. Accordingly, in the experiments performed at different speeds of the uneven mounted BLDC drone motor, the proposed network detected the fault with 100% accuracy. As a result, it has been proven that the proposed method detects the uneven mounting fault of the UAV BLDC motor cost-effectively with high accuracy.

5.1 Future scope of current work

It is planned to carry out the training and testing process entirely with raw data, with new data to be provided in future studies. This is going to increase the classification accuracy, reliability and generalizability of the proposed method. In subsequent studies, the development of the model will be continued by supporting the missing aspects.

Author Contributions The authors contributed equally to all parts of the article.

Data availability No datasets were generated or analysed during the current study.

Declarations

Conflict of interest The authors declare that there are no Conflict of interest or Conflict of interest related to this research. And no funding was received for this study. Ethics approval was not deemed necessary for this study. The authors contributed equally to the conception, design, and execution of the study.

References

1. Ghazali, M.H.M., Teoh, K., Rahiman, W.: A systematic review of real-time deployments of UAV-based LoRa communication network. IEEE Access **9**, 124817–124830 (2021)
2. Ghazali, M.H.M., Rahiman, W.: Vibration-based fault detection in drone using artificial intelligence. IEEE Sens. J. **22**(9), 8439–8448 (2022)
3. Chan, H., Woo, K.: Closed loop speed control of miniature brushless dc motors. J. Autom. Control Eng. **3**(4) (2015)
4. Chan, H.L., Woo, K.T.: Design and control of small quadcopter system with motor closed loop speed control. Int. J. Mech. Eng. Robot. Res. **4**(4), 287–292 (2015)
5. Ali, Z.A., Wang, D., Aamir, M.: Fuzzy-based hybrid control algorithm for the stabilization of a tri-rotor UAV. Sensors **16**(5), 652 (2016)
6. Werner, U.: Analysis of different vibration control strategies for soft mounted induction motors with sleeve bearings using active motor foot mounts. J. Appl. Math. Phys. **7**(3), 611–637 (2019)
7. Chen, G., Li, S., He, Q., Zhou, P., Zhang, Q., Yang, G., Lv, D.: Fault diagnosis of drone motors driven by current signal data with few samples. Meas. Sci. Technol. **35**(8), 086202 (2024)
8. Kilic, U., Unal, G.: Aircraft air data system fault detection and reconstruction scheme design. Aircr. Eng. Aerosp. Technol. **93**(6), 1104–1114 (2021)
9. Kilic, U., Unal, G.: Sensor fault detection and reconstruction system for commercial aircrafts. Aeronaut. J. **126**(1299), 889–905 (2022)
10. Kaya, Y., Kuncan, M., Akcan, E., Kaplan, K.: An efficient approach based on a novel 1D-LBP for the detection of bearing failures with a hybrid deep learning method. Appl. Soft Comput. **155**, 111438 (2024)
11. Akcan, E., Kuncan, M., Kaplan, K., Kaya, Y.: Diagnosing bearing fault location, size, and rotational speed with entropy variables using extreme learning machine. J. Braz. Soc. Mech. Sci. Eng. **46**(1), 4 (2024)
12. Glowacz, A.: Acoustic based fault diagnosis of three-phase induction motor. Appl. Acoust. **137**, 82–89 (2018)
13. Glowacz, A., Glowacz, W., Glowacz, Z., Kozik, J.: Early fault diagnosis of bearing and stator faults of the single-phase induction motor using acoustic signals. Measurement **113**, 1–9 (2018)
14. Ameid, T., Menacer, A., Talhaoui, H., Harzelli, I.: Broken rotor bar fault diagnosis using fast Fourier transform applied to field-oriented control induction machine: simulation and experimental study. Int. J. Adv. Manuf. Technol. **92**, 917–928 (2017)
15. Hosseini, S.M., Hosseini, F., Abedi, M.: Stator fault diagnosis of a BLDC motor based on discrete wavelet analysis using ADAMS simulation. SN Appl. Sci. **1**, 1–13 (2019)
16. Tian, Y., Guo, D., Zhang, K., Jia, L., Qiao, H., Tang, H.: A review of fault diagnosis for traction induction motor. In: 2018 37th Chinese Control Conference (CCC), pp. 5763–5768. IEEE (2018)
17. Contreras-Hernandez, J.L., Almanza-Ojeda, D.L., Ledesma-Orozco, S., Garcia-Perez, A., Romero-Troncoso, R.J., Ibarra-Manzano, M.A.: Quaternion signal analysis algorithm for induction motor fault detection. IEEE Trans. Ind. Electron. **66**(11), 8843–8850 (2019)
18. Ali, M.Z., Shabbir, M.N.S.K., Liang, X., Zhang, Y., Hu, T.: Machine learning-based fault diagnosis for single-and multi-faults in induction motors using measured stator currents and vibration signals. IEEE Trans. Ind. Appl. **55**(3), 2378–2391 (2019)
19. AlShorman, O., Alkahatni, F., Masadeh, M., Irfan, M., Glowacz, A., Althobiani, F., Kozik, J., Glowacz, W.: Sounds and acoustic emission-based early fault diagnosis of induction motor: a review study. Adv. Mech. Eng. **13**(2), 1687814021996915 (2021)
20. Lee, J.-H., Pack, J.-H., Lee, I.-S.: Fault diagnosis of induction motor using convolutional neural network. Appl. Sci. **9**(15), 2950 (2019)
21. Chang, H.-C., Jheng, Y.-M., Kuo, C.-C., Hsueh, Y.-M.: Induction motors condition monitoring system with fault diagnosis using a hybrid approach. Energies **12**(8), 1471 (2019)
22. Abed, W., Sharma, S., Sutton, R., Motwani, A.: A robust bearing fault detection and diagnosis technique for brushless dc motors

under non-stationary operating conditions. J. Control Autom. Electr. Syst. **26**, 241–254 (2015)
23. Shifat, T.A., Hur, J.-W.: ANN assisted multi sensor information fusion for BLDC motor fault diagnosis. IEEE Access **9**, 9429–9441 (2021)
24. Lee, J., Lee, W., Ko, S., Oh, H.: Fault classification and diagnosis of UAV motor based on estimated nonlinear parameter of steady-state model. Int. J. Mech. Eng. Robot. Res **10**, 22–31 (2020)
25. Bondyra, A., Gasior, P., Gardecki, S., Kasiński, A.: Fault diagnosis and condition monitoring of UAV rotor using signal processing. In: 2017 Signal Processing: Algorithms, Architectures, Arrangements, and Applications (SPA), pp. 233–238. IEEE (2017)
26. Pourpanah, F., Zhang, B., Ma, R., Hao, Q.: Anomaly detection and condition monitoring of UAV motors and propellers. In: 2018 IEEE Sensors, pp. 1–4. IEEE (2018)
27. Medeiros, R.L.V., Ramos, J.G.G.S., Nascimento, T.P., Lima Filho, A.C., Brito, A.V.: A novel approach for brushless DC motors characterization in drones based on chaos. Drones **2**(2), 14 (2018)
28. Iannace, G., Ciaburro, G., Trematerra, A.: Fault diagnosis for UAV blades using artificial neural network. Robotics **8**(3), 59 (2019)
29. Jesus Rangel-Magdaleno, J., Ureña-Ureña, J., Hernández, A., Perez-Rubio, C.: Detection of unbalanced blade on UAV by means of audio signal. In: 2018 IEEE International Autumn Meeting on Power, Electronics and Computing (ROPEC), pp. 1–5. IEEE (2018)
30. Veras, F.C., Lima, T.L., Souza, J.S., Ramos, J.G., Lima Filho, A.C., Brito, A.V.: Eccentricity failure detection of brushless dc motors from sound signals based on density of maxima. IEEE Access **7**, 150318–150326 (2019)
31. Liu, W., Chen, Z., Zheng, M.: An audio-based fault diagnosis method for quadrotors using convolutional neural network and transfer learning. In: 2020 American Control Conference (ACC), pp. 1367–1372. IEEE (2020)
32. Altinors, A., Yol, F., Yaman, O.: A sound based method for fault detection with statistical feature extraction in UAV motors. Appl. Acoust. **183**, 108325 (2021)
33. Yaman, O., Yol, F., Altinors, A.: A fault detection method based on embedded feature extraction and SVM classification for UAV motors. Microprocess. Microsyst. **94**, 104683 (2022)
34. Sonmez, E., Kacar, S., Uzun, S.: A new deep learning model combining CNN for engine fault diagnosis. J. Braz. Soc. Mech. Sci. Eng. **45**(12), 644 (2023)
35. Chollet, F.: Python ile derin öğrenme. Baskı ed. Buzdağı Yayınevi, Ankara, 129
36. Hoang, D.-T., Kang, H.-J.: A survey on deep learning based bearing fault diagnosis. Neurocomputing **335**, 327–335 (2019)
37. Cheng, C., Li, J., Liu, Y., Nie, M., Wang, W.: Deep convolutional neural network-based in-process tool condition monitoring in abrasive belt grinding. Comput. Ind. **106**, 1–13 (2019)
38. Hubner, H.B., Duarte, M.A.V., Silva, R.B.: Automatic grinding burn recognition based on time–frequency analysis and convolutional neural networks. Int. J. Adv. Manuf. Technol. **110**(7), 1833–1849 (2020)
39. Li, Y., Yang, Y., Wang, X., Liu, B., Liang, X.: Early fault diagnosis of rolling bearings based on hierarchical symbol dynamic entropy and binary tree support vector machine. J. Sound Vib. **428**, 72–86 (2018)
40. Pires, V.F., Foito, D., Martins, J., Pires, A.: Detection of stator winding fault in induction motors using a motor square current signature analysis (MSCSA). In: 2015 IEEE 5th International Conference on Power Engineering, Energy and Electrical Drives (POWERENG), pp. 507–512. IEEE (2015)
41. Jiao, J., Zhao, M., Lin, J., Liang, K.: A comprehensive review on convolutional neural network in machine fault diagnosis. Neurocomputing **417**, 36–63 (2020)
42. Xia, C.-L.: Permanent Magnet Brushless DC Motor Drives and Controls. Wiley, Hoboken (2012)
43. Mohanraj, D., Aruldavid, R., Verma, R., Sathiyasekar, K., Barnawi, A.B., Chokkalingam, B., Mihet-Popa, L.: A review of BLDC motor: state of art, advanced control techniques, and applications. IEEE Access **10**, 54833–54869 (2022)
44. Varanis, M., Silva, A., Mereles, A., Pederiva, R.: Mems accelerometers for mechanical vibrations analysis: a comprehensive review with applications. J. Braz. Soc. Mech. Sci. Eng. **40**, 1–18 (2018)
45. Hasibuzzaman, M., Shufian, A., Shefa, R.K., Raihan, R., Ghosh, J., Sarker, A.: Vibration measurement & analysis using Arduino based accelerometer. In: 2020 IEEE Region 10 Symposium (TENSYMP), pp. 508–512. IEEE (2020)
46. Iwaniec, M., Holovatyy, A., Teslyuk, V., Lobur, M., Kolesnyk, K., Mashevska, M.: Development of vibration spectrum analyzer using the raspberry pi microcomputer and 3-axis digital mems accelerometer adxl345. In: 2017 XIIIth International Conference on Perspective Technologies and Methods in MEMS Design (MEMSTECH), pp. 25–29. IEEE (2017)
47. Adli, B., Rusmin, P.H.: Vibration measuring tools for rotary pumping machine with accelerometer mems sensor. In: 2020 FORTEI-International Conference on Electrical Engineering (FORTEI-ICEE), pp. 69–74. IEEE (2020)
48. Elasha, F., Ruiz-Carcel, C., Mba, D., Jaramillo, V., Ottewill, J.: Detection of machine soft foot with vibration analysis. Insight-Non-Destr. Test. Cond. Monit. **56**(11), 622–626 (2014)
49. Pereira, V., Fernandes, V.A., Sequeira, J.: Low cost object sorting robotic arm using raspberry pi. In: 2014 IEEE Global Humanitarian Technology Conference-South Asia Satellite (GHTC-SAS), pp. 1–6. IEEE (2014)
50. Neupane, D., Seok, J.: Bearing fault detection and diagnosis using case western reserve university dataset with deep learning approaches: a review. IEEE Access **8**, 93155–93178 (2020)
51. Chen, J.J., Delongchamp, R.R., Tsai, C.-A., Hsueh, H.-M., Sistare, F., Thompson, K.L., Desai, V.G., Fuscoe, J.C.: Analysis of variance components in gene expression data. Bioinformatics **20**(9), 1436–1446 (2004)
52. Dinčić, M., Denić, D., Perić, Z.: Design and analysis of different techniques for analog-to-digital conversion of vibration signals for wireless measurement systems. Facta Univ. Ser. Autom. Control Robot. **17**(1), 39–56 (2018)
53. Feurer, M., Klein, A., Eggensperger, K., Springenberg, J.T., Blum, M., Hutter, F.: In: Hutter, F., Kotthoff, L., Vanschoren, J. (eds.) Auto-sklearn: Efficient and Robust Automated Machine Learning, pp. 113–134. Springer, Cham (2019)